Vibrational states of atomic hydrogen in bulk and nanocrystalline palladium studied by neutron spectroscopy

Maiko Kofu,[1,*] Naoki Hashimoto,[1] Hiroshi Akiba,[1] Hirokazu Kobayashi,[2] Hiroshi Kitagawa,[2] Kazuki Iida,[3] Mitsutaka Nakamura,[4] and Osamu Yamamuro[1,†]

[1]*Institute for Solid State Physics, University of Tokyo, Kashiwa, Chiba 277-8581, Japan*

[2]*Graduate School of Science, Kyoto University, Sakyo-ku, Kyoto 606-8502, Japan*

[3]*Research Center for Neutron Science and Technology, Comprehensive Research Organization for Science and Society, Tokai, Ibaraki 319-1106, Japan*

[4]*Materials and Life Science Division, J-PARC Center, Tokai, Ibaraki 319-1195, Japan*

(Received 27 March 2017; revised manuscript received 12 July 2017; published 24 August 2017)

The vibrational states of hydrogen atoms in bulk and nanocrystalline palladium were examined in a wide energy region $0 \leqslant \hbar\omega \leqslant 300$ meV using neutron spectroscopy. In bulk $PdH_{0.73}$, the vibrational excitations of H atoms were roughly reproduced by the quantum harmonic oscillator (QHO) model. In $PdH_{0.42}$ nanocrystals with a diameter of 8 nm, however, additional vibrational excitations were found at energies above 80 meV. The energies and intensities of the additional states were not explained by the QHO but reasonably described as vibrations in a highly anharmonic trumpetlike potential. The additional excitations are attributed to the vibrations of H atoms at tetrahedral sites in the subsurface region stabilized by surface effects. Thus, this is an experimental work which clearly detects hydrogen vibration *inside* metal nanoparticles.

DOI: 10.1103/PhysRevB.96.054304

I. INTRODUCTION

The behavior of hydrogen in metals has attracted much attention in fundamental and applied research areas. Palladium hydride (PdH_x) is a typical metal-hydrogen system and has been intensively studied for many decades. Pd has remarkable abilities to absorb plenty of hydrogen and to catalyze a broad range of chemical reactions. Metal nanoparticles are of current interest owing to their unique properties as compared with bulk materials [1–4]. It has been demonstrated that the H absorption properties of Pd nanoparticles are markedly different from that of bulk Pd and strongly depend on their size, shape, and surface structure [5–12]. The Pd nanoparticles with high surface area also offer high catalytic activity [13–16]. In the field of surface science, it has been often discussed that the potential energy for the H sites significantly changes near (a few layers below) the surface of a particle, which is usually called the "subsurface" [3,17–24]. A key issue in metal hydride nanoparticles is to clarify the thermodynamic state and structure of the subsurface which are closely connected with the H absorption ability and the high catalytic performance.

Bulk PdH_x undergoes a phase transition from a hydrogen dilute α phase to a concentrated, lattice expanded β phase. In both phases, the H atoms occupy the interstitial octahedral (O) sites $(1/2,1/2,1/2)$ in the face-centered cubic (fcc) Pd lattice [25–35] (see Fig. 1). Our recent neutron diffraction (ND) work on nanocrystalline PdD_x (nano-PdD_x) demonstrated that some of H atoms, probably in the subsurface, are accommodated at the tetrahedral (T) sites $(1/4,1/4,1/4)$ [36]. It was also reported by a quasielastic neutron scattering (QENS) study that an additional fast diffusion process of the H atoms appeared in nano-PdH_x [37]. These results suggest that the H atoms diffuse faster near the surface, probably via the T sites.

Inelastic neutron scattering (INS) spectroscopy is a powerful technique in probing vibrational states of H atoms in metal lattices. The precise analysis of INS spectra enables us to predict the potential surface around the H atom position. With this view, a number of INS measurements have been performed for bulk PdA_x (A = H, D, T) so far [38–48]. They have demonstrated that the optical H vibrations in PdH_x are rather anisotropic and anharmonic [47,48], which is consistent with the theoretical prediction of *ab initio* calculations [49]. Stuhr *et al.* have made INS measurements up to 140 meV for nano-PdH_x ($x \leqslant 0.048$) with a diameter of smaller than 23 nm [50]. The vibrational excitations, which are attributed to the H atoms near the grain boundary, were observed in the energy region between 90 and 140 meV. They also found an excitation peak at 50–80 meV which resembles that observed in bulk PdH_x.

Here we report an INS study of bulk $PdH_{0.73}$ and high-quality nano-$PdH_{0.42}$ with a smaller and more uniform diameter (8.0 ± 0.9 nm) than in the previous study [50]. The vibrational dynamics of H atoms were investigated in the wide energy-transfer region $0 \leqslant \hbar\omega \leqslant 300$ meV using a modern sophisticated neutron spectrometer, to gain insight into the shape of the potential well for hydrogen vibration in the subsurface. Our nanocrystals are capped by a protective polymer, polyvinylpyrrolidone (PVP), and are isolated from each other, in contrast to the Stuhr's nanoparticles. We do not suffer from H atoms in grain boundaries. Thus, this is an experimental work on hydrogen vibration inside metal nanoparticles.

II. EXPERIMENT

The Pd powder used as a bulk sample was obtained from Sigma Aldrich with a specified purity of 99.9% and the

*Present address: Materials and Life Science Division, J-PARC Center, Tokai, Ibaraki 319-1195, Japan; maiko.kofu@j-parc.jp

†yamamuro@issp.u-tokyo.ac.jp

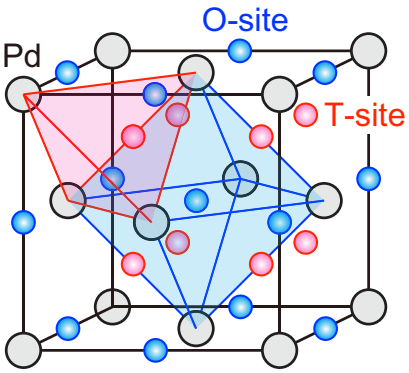

FIG. 1. Locations of interstitial hydrogen atoms in an fcc Pd lattice; octahedral (O) and tetrahedral (T) sites.

hydrogen gas (purity 99.99%) from Suzuki Shokan. The Pd nanocrystals used in this work are basically the same as those in the previous heat capacity [51], neutron diffraction [36], and QENS measurements [37]. The nanocrystals were synthesized by the same method described elsewhere [52]. The mass ratio of Pd and PVP was determined to be 68:32, corresponding to the Pd volume fraction of 0.175. The sample amounts of the Pd powder and the nanocrystals (including PVP) were ca. 6 g and 2 g, respectively. The pretreatment and hydrogenation of the samples and the determination of H concentrations were carried out as described in Ref. [37]. The dehydrogenated Pd nanocrystals which were measured to estimate the effect of PVP were prepared by evacuating the nano-PdH sample at 100 °C. The samples were loaded into annular aluminum cells with a thickness of 0.5–1 and a diameter of 18 mm.

Neutron spectra of bulk $PdH_{0.73}$, nano-Pd, and nano-$PdH_{0.42}$ were recorded at 10 K using a time-of-flight Fermi chopper spectrometer, 4SEASONS [53], at the Japan Proton Accelerator Research Complex (J-PARC). The spectrometer has a unique ability to record the scattering events for neutrons with multiple incident energies E_i simultaneously [54]. The frequency of a Fermi chopper was set to 600 Hz and the phase was configured to select an E_i set of 942, 331, and 168 meV. Here we do not show the data obtained with $E_i = 942$ meV because the phonon excitations were not separated well due to the coarse energy resolution. The empty cell was measured to subtract scattering contributions from the instrument and the cell. The temperature of the samples was controlled by using a top-loading closed cycle refrigerator. The data reduction was done with Utsusemi software package [55] developed in J-PARC.

III. RESULTS AND DISCUSSION

A. Dynamical structure factors

Figure 2 shows color contour maps of the dynamical structure factor $S(Q,\omega)$ for bulk $PdH_{0.73}$ and nano-$PdH_{0.42}$, obtained with $E_i = 331$ meV at 10 K. Here the contribution from the empty cell and an instrumental background were already subtracted. As for nano-$PdH_{0.42}$, the nano-Pd data were also subtracted. The amount of H atoms in PVP is nine times larger than that in nano-$PdH_{0.42}$. The subtraction of scattering from PVP is necessary to extract vibrational excitations of H atoms in Pd. Figure 3 presents the actual process of the subtraction for the data integrated over limited Q regions. In fact, the observed $S(Q,\omega)$ of nano-$PdH_{0.42}$ and nano-Pd include a large scattering contribution from PVP as seen in Fig. 3. The several peaks between 100 and 140 meV are assigned to the vibration of the C-C bonds in the pyrrolidone ring and the strong broad band at around 170 meV to the carbonyl (C=O) stretch [56]. It is emphasized that the peaks disappear in the subtracted data (filled circles in Fig. 3), indicating successful subtraction.

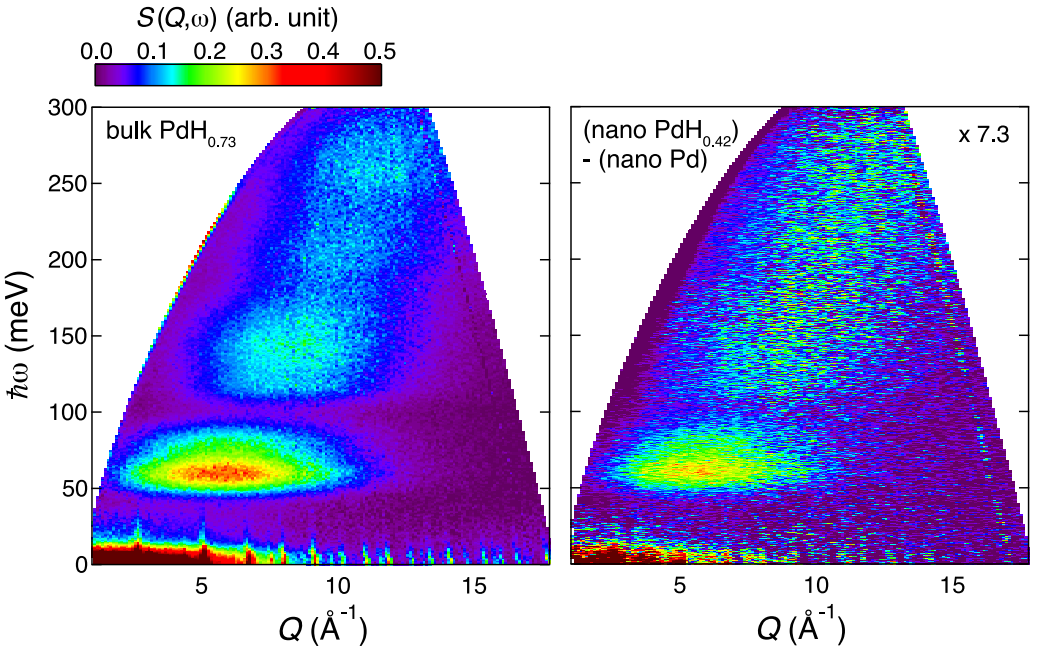

FIG. 2. Dynamical structure factors as functions of energy $\hbar\omega$ and momentum transfer Q for bulk and nano-PdH_x recorded at 10 K. The scattering contribution from nano-Pd has been subtracted from nano-$PdH_{0.42}$. The data were obtained with $E_i = 331$ meV.

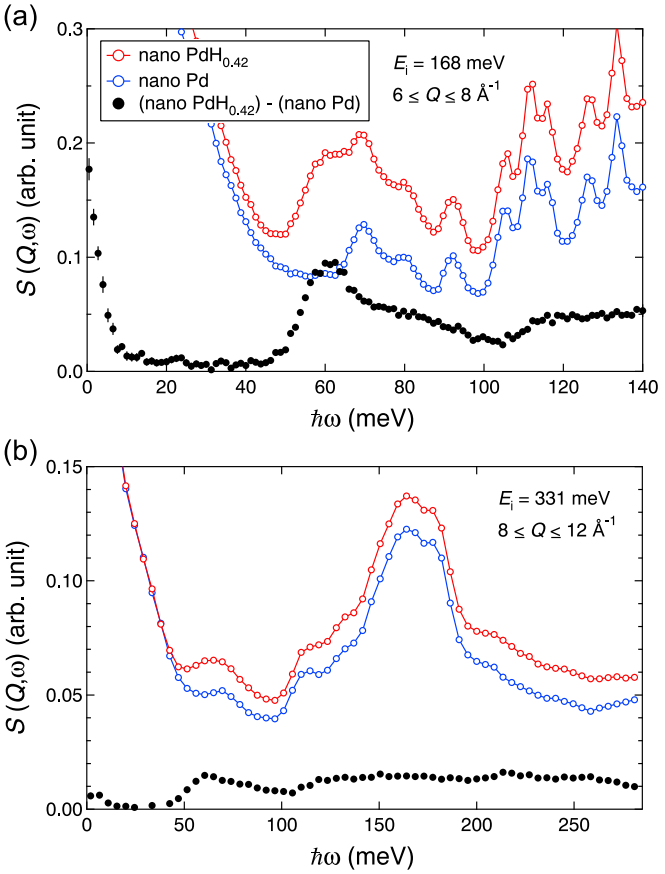

FIG. 3. Inelastic neutron scattering spectra of nano-$PdH_{0.42}$ and nano-Pd, recorded with E_i's of (a) 168 and (b) 331 meV at 10 K. The differences between the two spectra, (nano-$PdH_{0.42}$) − (nano-Pd), are also shown.

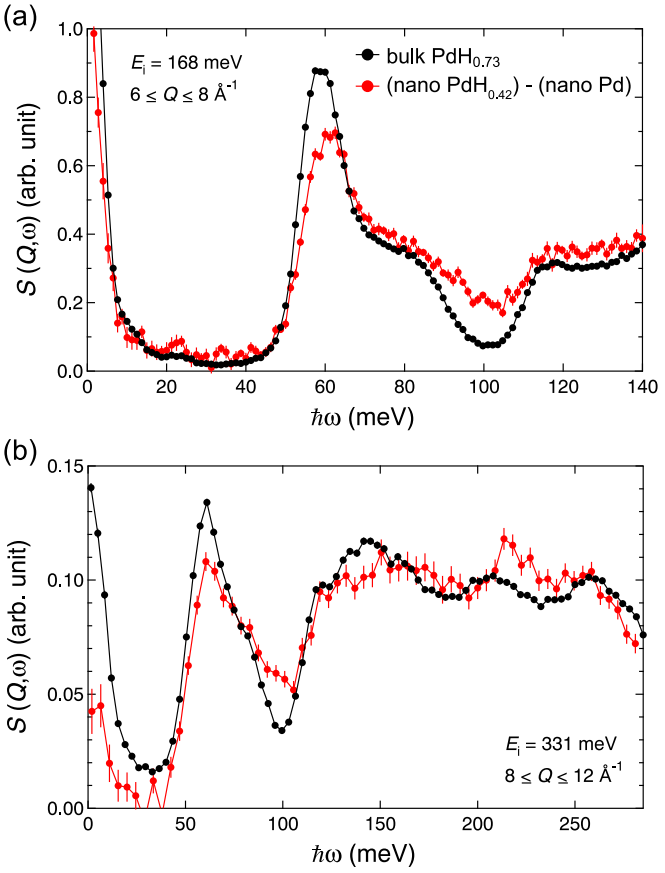

FIG. 4. Inelastic neutron scattering spectra of bulk $PdH_{0.73}$ and nano-$PdH_{0.42}$ recorded with E_i's of (a) 168 and (b) 331 meV. The data of nano-$PdH_{0.42}$, from which the scattering contribution from nano-Pd is subtracted, are multiplied by 7.3 for a comparison purpose.

Vibrational excitations are clearly visible at around 70, 140, 210, and 280 meV in bulk $PdH_{0.73}$. On the other hand, the $S(Q,\omega)$ map of nano-$PdH_{0.42}$ exhibits a clear excitation at 70 meV and a continuous excitation above 120 meV. The vibration of the host Pd lattice mainly reflects acoustic phonons which appear below 26 meV [40,47]. The excitations observed above 50 meV correspond to multiphonon processes that originate in the vibrations of H atoms.

Figure 4 displays the comparisons in INS spectra between bulk $PdH_{0.73}$ and nano-$PdH_{0.42}$. The spectrum of nano-$PdH_{0.42}$ exhibits the first excitation peak at around 60 meV as in the case of bulk $PdH_{0.73}$. A significant difference on the spectra is seen in the higher energy region. Additional excitations clearly appear above 80 meV in nano-$PdH_{0.42}$. It is noted that the position of the first peak slightly shifts toward a higher energy side in nano-$PdH_{0.42}$, suggesting that the vibrational mode hardens. From the spectrum with $E_i = 168$ meV, the peak position was estimated to be 59.3 meV which is 3% higher than that observed in bulk. The hardening could be related to the fact that the lattice constant of nano-$PdH_{0.42}$ is smaller than that of bulk $PdH_{0.73}$ [36]. It is also found that the vibrational excitations become broader in the nanocrystalline sample, implying an inhomogeneity of potential at H sites inside the nanoparticle.

B. Analysis for bulk PdH_x

In order to quantify the peak positions and areas, the INS spectra of bulk $PdH_{0.73}$ were fitted with multiple Gaussians $G_{n,i}(\omega)$,

$$S(Q,\omega)_{\text{bulk}} = \sum_n A_n \sum_i f_{n,i} G_{n,i}(\omega),$$
$$G_{n,i}(\omega) = \sqrt{\frac{\ln 2}{\pi}} \frac{1}{\Gamma_{n,i}} e^{-\ln 2\left(\frac{\hbar\omega - E_{n,i}}{\Gamma_{n,i}}\right)^2}, \quad (1)$$

with a constraint of $\sum_i f_{n,i} = 1$. Here the Gaussians were used to approximately describe the spectra. $E_{n,i}$ and $\Gamma_{n,i}$ are the position of the center and the half-width at half maximum (HWHM) of each peak, respectively.

We first analyzed the data obtained with $E_i = 168$ meV to characterize the fundamental ($n = 1$) excitation mode. The data in an energy range between 34 and 122 meV were fitted with four Gaussians; the fourth one is for $n = 2$. The result of the fit is shown as a solid curve in Fig. 5. The positions of the three peaks for $n = 1$ were 57.9, 65.6, and 81.5 meV. Next, advanced multipeak fitting was carried out for the spectrum with $E_i = 331$ meV [see Fig. 6(a)]. Nine Gaussian functions were used to reproduce the vibrational spectrum up to the $n = 5$ oscillator mode. The individual peaks are displayed as dashed curves. The positions and widths of the first three peaks

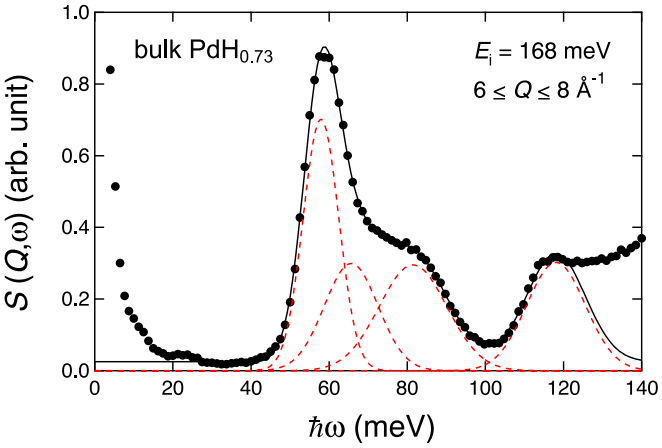

FIG. 5. Inelastic neutron scattering spectrum of bulk $PdH_{0.73}$ with $E_i = 168$ meV at 10 K. Solid curve represents the result of the fit with multiple Gaussians. The dashed curves correspond to each Gaussian function.

($n = 1$ mode) were fixed to the values obtained from the fit for the data with $E_i = 168$ meV.

In the quantum harmonic oscillator (QHO) model [57], the scattering intensity and energy for the nth excitation are given by

$$A_n \propto e^{-\langle u^2\rangle Q^2}(\langle u^2\rangle Q^2)^n/n!,$$
$$E_n - E_0 = n\hbar\omega_0, \tag{2}$$

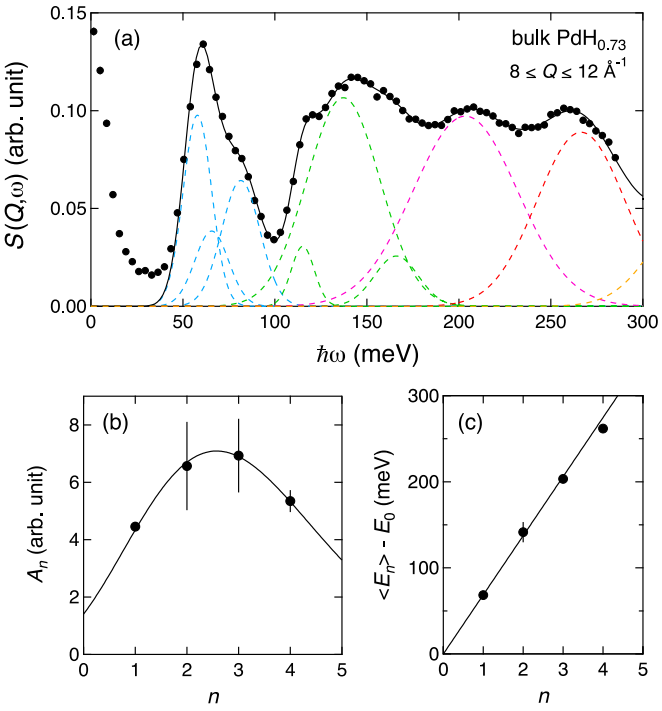

FIG. 6. (a) Inelastic neutron scattering spectrum for bulk $PdH_{0.73}$ at 10 K. The cyan, green, magenta, red, and orange dashed curves correspond to the $n = 1$, 2, 3, 4, 5 excitation modes, respectively. (b) Intensity and (c) excitation energy against quantum number n.

where $\langle u^2\rangle$ ($=\hbar/2m\omega_0$) is the mean square displacement of zero-point vibration and ω_0 the fundamental frequency. $n!$ is replaced by the Gamma function $\Gamma(n+1)$ in a practical manner. Based on the QHO model, the peak position, width, and area of the $n = 5$ mode were assumed as $(E_5 - E_0) = 5/4(E_4 - E_0)$, $\gamma_5 = \gamma_4$, and $A_5 = 0.656A_4$. These constraints were needed to analyze the excitation modes with $n \leqslant 4$ properly.

Figures 6(b) and 6(c) present A_n and the "averaged" excitation energy against n. The averaged energies for $n = 1,2$ were calculated as follows:

$$\langle E_n\rangle - E_0 = \sum_i f_{n,i} E_{n,i}, \tag{3}$$

where $f_{n,i}$ and $E_{n,i}$ are the same as those in Eq. (1).

The intensity and energy are sufficiently described by the QHO model, as shown by solid curves in Figs. 6(b) and 6(c). From the fit with Eq. (2), $\langle u^2\rangle$ and $\hbar\omega_0$ were estimated to be 0.0308(3) $Å^2$ and 68.7(9) meV, respectively. In the QHO model, the relation $\langle u^2\rangle = \hbar/2m\omega_0$ holds at low temperature. $\langle u^2\rangle$ is evaluated to be 0.0304 $Å^2$ for $\hbar\omega_0 = 68.7$ meV and is in excellent agreement with the above value from the fitting.

We now discuss the splitting of the excitation bands. The first band consists of a peak centered at 58 and a shoulder at 81 meV (see Fig. 5). In terms of H-H interactions, the main peak is ascribed to a transverse optical mode, while the high-energy shoulder to a longitudinal one [47], The peak positions are consistent with the dispersion relation measured by INS [40,44]. However there is another interpretation; namely, the shoulder is a transition to the Franck-Condon level in the frozen Pd lattice, or without consideration of the lattice relaxation in the excited states [48,58]. The origin of the shoulder is still an open problem but is beyond the scope of this paper.

The split of the second band is considered to be due to anharmonic effects [43,47–49]. For the three-dimensional isotropic harmonic oscillator, the Cartesian eigenstates $|n_x n_y n_z\rangle$ of the energy level n ($=n_x + n_y + n_z$) are $\frac{1}{2}(n+1)(n+2)$-fold degenerate. The fourth-order anharmonic terms can lift the degeneracy of the states with $n \geqslant 2$. In fact, the $n = 2$ state splits into three levels. The peak positions of the second band were estimated to be 115, 137, and 167 meV, which are in reasonable agreement with the literature values [48]. As for the third and fourth excitation modes, the peak splitting was not clearly seen and the excitations were represented as single broad peaks. It should be stressed here that the averaged energy of the n state is the same as that for the QHO within the framework of the perturbation theory. Additionally, the anisotropy in the INS spectra [47,48], which manifests itself by the anharmonicity, is not prominent in powder samples.

C. Analysis for nano-PdH_x

Figure 7(a) shows the INS spectrum of nano-$PdH_{0.42}$. The spectrum was fitted with the combination of the spectrum of the bulk $PdH_{0.73}$ (dashed curve) and the additional excitations (solid curves),

$$S(Q,\omega)_{\text{nano}} = b_0 S(Q,\omega)_{\text{bulk}} + b_1 S(Q,\omega)_{\text{add}},$$
$$S(Q,\omega)_{\text{add}} = \sum_{n'} A_{n'} G_{n'}(\omega). \tag{4}$$

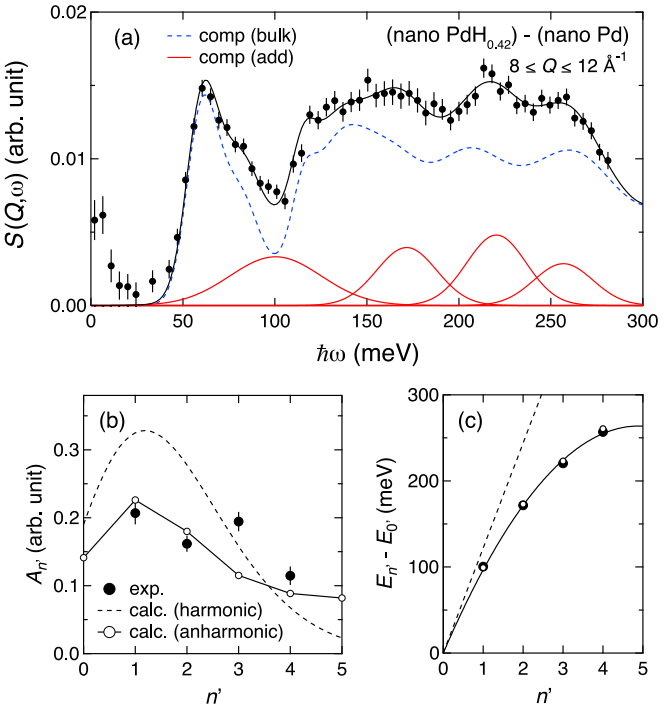

FIG. 7. (a) Inelastic neutron scattering spectrum for nano-$PdH_{0.42}$ at 10 K. The scattering contribution from nano-Pd is subtracted. (b) Intensity and (c) excitation energy against a quantum number n'.

The additional component was represented by multiple Gaussians $G_{n'}(\omega)$. In the fitting analysis, the parameters for $S(Q,\omega)_{\rm bulk}$ were fixed to be the same as those obtained for bulk $PdH_{0.73}$, except the 1_1 mode. As stated in Sec. III A, the 1_1 mode slightly hardens in nano-$PdH_{0.42}$. The parameters for the mode were estimated from the fit of the spectrum taken with $E_{\rm i} = 168$ meV. Thus, the parameters to be determined in the fitting were the prefactors b_0, b_1, areas, peak positions, and widths of $S(Q,\omega)_{\rm add}$; the widths for the $n = 2, 3, 4$ excitations are constrained to be the same. The fraction of the additional component, $b_1/(b_0 + b_1)$, was estimated to be 0.22. The value is consistent with the fraction of D atoms occupying the T site ($\approx$0.25 at 44 K) estimated from the neutron diffraction study [36]. It is naturally concluded that the bulklike excitations are the vibrations of H atoms at the O sites mainly in the interior region while the additional one originates from the H atoms at the T sites in the subsurface. The stability of the T site should depend on the mass (H or D) due to the zero-point energy. However, we consider that this isotope effect is not so serious to demolish this conclusion. Of course it is necessary to conduct the ND experiment for nano-PdH_x though it is very difficult because of small coherent and larger incoherent scattering cross sections of a H atom.

The estimated intensities and averaged excitation energies are displayed in Figs. 7(b) and 7(c). Dashed curves represent the expectation from the QHO model with $\hbar\omega_0 = 122$ meV. Obviously, the QHO model does not reproduce the experimental results. In order to characterize the additional states, anharmonicity should be considered.

Finally, we discuss the anharmonic potential by a simple numerical method. We assumed a one-dimensional symmetric

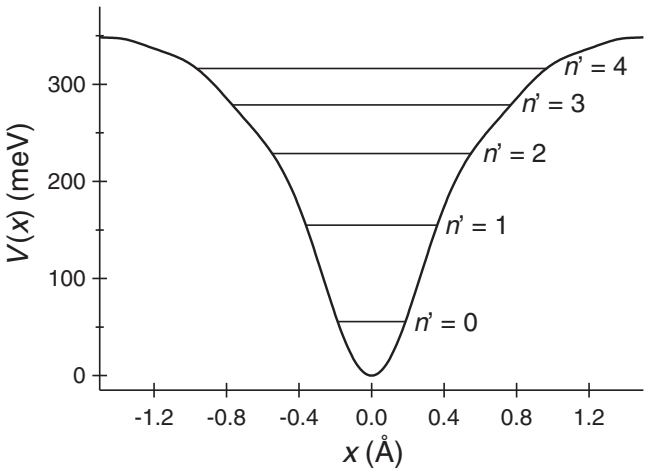

FIG. 8. Potential energy as a function of the atomic displacements relative to the equilibrium position of the H atom. The curve is calculated using Eq. (5). The parameters ω_0 and c_{2i} used in the calculation are summarized in Table. I. Horizontal lines represent the eigenvalues $E_{n'}$.

polynomial function

$$V(x) = \frac{1}{2}m\omega_0 x^2 + \sum_{i=2}^{10} c_{2i}x^{2i}. \quad (5)$$

The first term is just the QHO potential for which an exact analytical solution is known. Therefore, the 20 lowest wave functions for the QHO were chosen as a basis set in our calculation. By diagonalizing the Hamiltonian, $\mathcal{H} = -\frac{\hbar^2}{2m}\frac{d^2}{dx^2} + V(x)$, eigenvalues $E_{n'}$ and eigenstates $\psi_{n'}$ for the anharmonic potential were obtained. The scattering intensities were calculated with the following formula:

$$A_{n'} \propto \left| \int_{-\infty}^{\infty} \psi_{n'} e^{iQx} \psi_0 dx \right|^2. \quad (6)$$

These calculations were carried out using scripts written in *Mathematica* 10.4 software (Wolfram Research).

Open circles in Figs. 7(b) and 7(c) are the calculated values with assuming the potential surface shown in Fig. 8. The reasonable agreement is obtained between the experiment and calculation. The large deviation at $n' = 3$ could be due to the presence of vibration of H atoms on the Pd surface. The deduced potential surface is highly anharmonic and of trumpetlike shape, in contrast to the nearly harmonic potential in bulk $PdH_{0.73}$. The potential is steep at lower energies while rather gentle at higher energies. Compared with the harmonic model, $A_{n'}$, which reflects the spatial distribution of the wave functions, represents a larger value for larger n.

TABLE I. Parameters for the anharmonic potential, $V(x) = \frac{1}{2}m\omega_0 x^2 + \sum_{i=2}^{10} c_{2i}x^{2i}$. All values are in meV.

$\hbar\omega_0 = 122$ meV	$c_{12} = -4864.1$ meV/Å^2
$c_4 = -5970$ meV/Å^2	$c_{14} = 1257$ meV/Å^2
$c_6 = 12\,054$ meV/Å^2	$c_{16} = -151.01$ meV/Å^2
$c_8 = -14\,593$ meV/Å^2	$c_{18} = -0.38007$ meV/Å^2
$c_{10} = 10\,802$ meV/Å^2	$c_{20} = 1.2804$ meV/Å^2

The fundamental energy $\hbar\omega_0$ was estimated to be 122 meV which is significantly larger than that of bulk $PdH_{0.73}$. The vibrational mode comes from the H atom in a steep potential. Such a remarkable change in ω_0 cannot be explained by the change in the lattice constant. The present analysis suggests that the distance between H and Pd atoms is rather short. In fact, the H-Pd distance is 2 Å for the *O* site and 1.73 Å for the *T* site. The observation of the vibrational modes with high fundamental energy also supports our conclusion that some of the H atoms are accommodated at the *T* sites in the nanoparticles. It has been pointed out that the vibrational energy (or zero point energy) at the *T* site is higher than that at the *O* site [49,59,60]. However, the anharmonicity is not predicted for the *T* site in bulk PdH_x. We argue that the newly appeared vibrational states with strong anharmonicity in nano-$PdH_{0.42}$ are characteristic of the H atoms at the *T* site in the subsurface. The strong modification of potential could be caused by surface strain/distortion effects of nanoparticles.

IV. SUMMARY

Vibrational spectra of hydrogen in bulk and nanocrystalline Pd were investigated by inelastic neutron scattering in the energy range up to 300 meV. The spectrum of bulk $PdH_{0.73}$ is roughly described by quantum harmonic oscillators. In $PdH_{0.42}$ nanocrystals with a diameter of 8 nm, the excess excitations were found at higher energies in addition to the excitations which closely resemble those observed in bulk $PdH_{0.73}$. Our analysis demonstrated that the excess excitations are attributed to the hydrogen vibrations in a highly anharmonic trumpetlike potential which is realized at the *T* sites in the subsurface region. Further theoretical calculations on the actual three-dimensional nanocrystal are needed to reveal the details of vibrational states.

ACKNOWLEDGMENTS

This work was supported by CREST, Japan Science and Technology Agency. We thank Prof. S. Ikeda for fruitful discussions, and Dr. R. Kajimoto and Dr. Y. Inamura for their help in the experiment on 4SEASONS. The experiment in the Materials and Life Science Experimental Facility at J-PARC was performed with the approval of J-PARC (Proposal No. 2015A0260).

[1] G. Schmid, *Clusters and Colloids* (VCH, Weinheim, 1994).
[2] Y. Volokitin, J. Sinzig, L. J. de Jongh, G. Schmid, M. N. Vargaftik, and I. I. Moiseevi, Nature (London) **384**, 621 (1996).
[3] A. Pundt and R. Kirchheim, Annu. Rev. Mater. Res. **36**, 555 (2006).
[4] J. M. Campelo, D. Luna, R. Luque, J. M. Marinas, and A. A. Romero, ChemSusChem **2**, 18 (2009).
[5] R. J. Wolf, M. W. Lee, and J. R. Ray, Phys. Rev. Lett. **73**, 557 (1994).
[6] C. Sachs, A. Pundt, R. Kirchheim, M. Winter, M. T. Reetz, and D. Fritsch, Phys. Rev. B **64**, 075408 (2001).
[7] V. Bérubé, G. Radtke, M. Dresselhaus, and G. Chen, Int. J. Energy Res. **31**, 637 (2007).
[8] M. Yamauchi, R. Ikeda, H. Kitagawa, and M. Takata, J. Phys. Chem. C **112**, 3294 (2008).
[9] R. Bardhan, L. O. Hedges, C. L. Pint, A. Javey, S. Whitelam, and J. J. Urban, Nat. Mater. **12**, 905 (2013).
[10] G. Li, H. Kobayashi, J. M. Taylor, R. Ikeda, Y. Kubota, K. Kato, M. Takata, T. Yamamoto, S. Toh, S. Matsumura, and H. Kitagawa, Nat. Mater. **13**, 802 (2014).
[11] G. Li, H. Kobayashi, S. Dekura, R. Ikeda, Y. Kubota, K. Kato, M. Takata, T. Yamamoto, S. Matsumura, and H. Kitagawa, J. Am. Chem. Soc. **136**, 10222 (2014).
[12] R. Griessen, N. Strohfeldt, and H. Giessen, Nat. Mater. **15**, 311 (2015).
[13] D. Teschner, J. Borsodi, A. Wootsch, Z. Révay, M. Hävecker, A. Knop-Gericke, S. D. Jackson, and D. Schlögl, Science **320**, 86 (2008).
[14] A. Mohanty, N. Garg, and R. Jin, Angew. Chem., Int. Ed. Engl. **49**, 4962 (2010).
[15] S. Ogura, M. Okada, and K. Fukutani, J. Phys. Chem. C **119**, 23973 (2015).
[16] J. Mondal, Q. T. Trinh, A. Jana, W. K. H. Ng, P. Borah, H. Hirao, and Y. Zhao, ACS Appl. Mater. Interfaces **8**, 15307 (2016).
[17] K. H. Rieder, M. Baumberger, and W. Stocker, Phys. Rev. Lett. **51**, 1799 (1983).
[18] R. J. Behm, V. Penka, M.-G. Cattania, K. Christmann, and G. Ertl, J. Chem. Phys. **78**, 7486 (1983).
[19] H. Okuyama, W. Siga, N. Takagi, M. Nishijima, and T. Aruga, Surf. Sci. **401**, 344 (1998).
[20] M. Wilde and K. Fukutani, Phys. Rev. B **78**, 115411 (2008).
[21] M. Wilde, K. Fukutani, M. Naschitzki, and H. J. Freund, Phys. Rev. B **77**, 113412 (2008).
[22] S. Wilke, D. Hennig, and R. Löber, Phys. Rev. B **50**, 2548 (1994).
[23] J.-F. Paul and P. Sautet, Phys. Rev. B **53**, 8015 (1996).
[24] N. Ozawa, N. B. Arboleda, Jr., T. A. Roman, H. Nakanishi, W. A. Diño, and H. Kasai, J. Phys.: Condens. Matter **19**, 365214 (2007).
[25] J. E. Worsham, M. K. Wilkinson, and C. G. Shull, J. Phys. Chem. Solids **3**, 303 (1957).
[26] G. A. Ferguson, A. J. Schindler, T. Tanaka, and T. Morita, Phys. Rev. **137**, A483 (1965).
[27] G. Nelin, Phys. Status Solidi **45**, 527 (1971).
[28] I. S. Anderson, C. J. Carlile, and D. K. Ross, J. Phys. C **11**, L381 (1978).
[29] O. Blaschko, R. Klemencic, P. Weinzierl, and O. Eder, Solid State Commun. **27**, 1149 (1978).
[30] T. E. Ellis, C. B. Satterthwaite, M. H. Mueller, and T. O. Brun, Phys. Rev. Lett. **42**, 456 (1979).
[31] O. Blaschko, R. Klemencic, P. Weinzierl, and O. Eder, Acta Crystallogr. Sect. A **36**, 605 (1980).
[32] S. J. Kennedy, E. Wu, E. H. Kisi, E. M. Gray, and B. J. Kennedy, J. Phys.: Condens. Matter **7**, L33 (1995).

[33] E. Wu, S. J. Kennedy, E. M. Gray, and E. H. Kisi, J. Phys.: Condens. Matter **8**, 2807 (1996).
[34] M. Pitt and E. M. Gray, Europhys. Lett. **64**, 344 (2003).
[35] K. G. McLennan, E. M. Gray, and J. F. Dobson, Phys. Rev. B **78**, 014104 (2008).
[36] H. Akiba, M. Kofu, H. Kobayashi, H. Kitagawa, K. Ikeda, T. Otomo, and O. Yamamuro, J. Am. Chem. Soc. **138**, 10238 (2016).
[37] M. Kofu, N. Hashimoto, H. Akiba, H. Kobayashi, H. Kitagawa, M. Tyagi, A. Faraone, J. R. D. Copley, W. Lohstroh, and O. Yamamuro, Phys. Rev. B **94**, 064303 (2016).
[38] J. Bergsma and J. A. Goedkoop, Physica (Amsterdam) **26**, 744 (1960).
[39] M. R. Chowdhury and D. K. Ross, Solid State Commun. **13**, 229 (1973).
[40] J. M. Rowe, J. J. Rush, H. G. Smith, M. Mostoller, and H. E. Flotow, Phys. Rev. Lett. **33**, 1297 (1974).
[41] A. Rahman, K. Sköld, C. Pelizzari, S. K. Sinha, and H. Flotow, Phys. Rev. B **14**, 3630 (1976).
[42] W. Drexel, A. Murani, D. Tocchetti, W. Kley, I. Sosnowska, and D. K. Ross, J. Phys. Chem. Solids **37**, 1135 (1976).
[43] J. J. Rush, J. M. Rowe, and D. Richter, Z. Phys. B **55**, 283 (1984).
[44] J. M. Rowe, J. J. Rush, J. E. Schirber, and J. M. Mintz, Phys. Rev. Lett. **57**, 2955 (1986).
[45] A. I. Kolesnikov, I. Natkaniec, V. E. Antonov, I. T. Belash, V. K. Fedotov, J. Krawczyk, J. Mayer, and E. G. Ponyatovsky, Physica B (Amsterdam) **174**, 257 (1991).
[46] Y. Nakai, E. Akiba, H. Asano, and S. Ikeda, J. Phys. Soc. Jpn. **61**, 1834 (1992).
[47] D. K. Ross, V. E. Antonov, E. L. Bokhenkov, A. I. Kolesnikov, E. G. Ponyatovsky, and J. Tomkinson, Phys. Rev. B **58**, 2591 (1998).
[48] M. Kemali, J. E. Totolici, D. K. Ross, and I. Morrison, Phys. Rev. Lett. **84**, 1531 (2000).
[49] C. Elsässer, K. M. Ho, C. T. Chan, and M. Fähnle, J. Phys.: Condens. Matter **4**, 5207 (1992).
[50] U. Stuhr, H. Wipf, T. J. Udovic, J. Weißmüller, and H. Gleiter, J. Phys.: Condens. Matter **7**, 219 (1995).
[51] H. Akiba, H. Kobayashi, H. Kitagawa, M. Kofu, and O. Yamamuro, Phys. Rev. B **92**, 064202 (2015).
[52] B. Lim, M. Jiang, P. H. C. Camargo, E. C. Cho, J. Tao, X. Lu, Y. Zhu, and Y. Xia, Science **324**, 1302 (2009).
[53] R. Kajimoto *et al.*, J. Phys. Soc. Jpn. **80**, SB025 (2011).
[54] M. Nakamura, R. Kajimoto, Y. Inamura, F. Mizuno, M. Fujita, T. Yokoo, and M. Arai, J. Phys. Soc. Jpn. **78**, 093002 (2009).
[55] Y. Inamura, T. Nakatani, J. Suzuki, and T. Otomo, J. Phys. Soc. Jpn. **82**, SA031 (2013).
[56] Y. Borodko, S. E. Habas, M. Koebel, P. Yang, H. Frei, and G. A. Somorjai, J. Phys. Chem. B **110**, 23052 (2006).
[57] S. W. Lovesey, *Theory of Neutron Scattering from Condensed Matter* (Clarendon, Oxford, 1984), Vol. 1.
[58] H. Krimmel, L. Schimmele, C. Elsässer, and M. Fähnle, J. Phys.: Condens. Matter **6**, 7679 (1994).
[59] R. Caputo and A. Alavi, Mol. Phys. **101**, 1781 (2003).
[60] C. Wei, F. T. Kong, and H. R. Gong, Int. J. Hydrog. Energy **38**, 16485 (2013).